

# A Reservoir of *Moraxella catarrhalis* in Human Pharyngeal Lymphoid Tissue

Nadja Heiniger,<sup>1</sup> Violeta Spaniol,<sup>1</sup> Rolf Troller,<sup>1</sup> Mattheus Vischer,<sup>2</sup> and Christoph Aebi<sup>1,3</sup>

<sup>1</sup>Institute for Infectious Diseases and Departments of <sup>2</sup>Otorhinolaryngology and <sup>3</sup>Pediatrics, University of Bern, Switzerland

**Background.** Early exposure of infants and long-term immunity suggest that colonization with *Moraxella catarrhalis* is more frequent than is determined by routine culture. We characterized a reservoir of *M. catarrhalis* in pharyngeal lymphoid tissue.

**Methods.** Tissue from 40 patients (median age, 7.1 years) undergoing elective tonsillectomy and/or adenoidectomy was analyzed for the presence of *M. catarrhalis* by culture, real-time DNA and RNA polymerase chain reaction (PCR), immunohistochemical analysis (IHC), and fluorescent in situ hybridization (FISH). Histologic sections were double stained for *M. catarrhalis* and immune cell markers, to characterize the tissue distribution of the organism. Intracellular bacteria were identified using confocal laser scanning microscopy (CLSM).

**Results.** Twenty-nine (91%) of 32 adenoids and 17 (85%) of 20 tonsils were colonized with *M. catarrhalis*. Detection rates for culture, DNA PCR, RNA PCR, IHC, and FISH were 7 (13%) of 52, 10 (19%) of 52, 21 (41%) of 51, 30 (61%) of 49, and 42 (88%) of 48, respectively ( $P < .001$ ). Histologic analysis identified *M. catarrhalis* in crypts, intraepithelially, subepithelially, and (using CLSM) intracellularly. *M. catarrhalis* colocalized with macrophages and B cells in lymphoid follicles.

**Conclusions.** Colonization by *M. catarrhalis* is more frequent than is determined by surface culture, because the organism resides both within and beneath the epithelium and invades host cells.

*Moraxella catarrhalis* is a respiratory-tract commensal organism and a major cause of otitis media in children. Its contribution to the total disease burden brought about by otitis media will increase in the near future, because the routine use of pneumococcal conjugate vaccines is associated with an increase in nasopharyngeal colonization rates [1] and episodes of otitis media caused by *M. catarrhalis* and other organisms [2, 3]. This emergent role of *M. catarrhalis* calls for intensified efforts to understand its interaction with the human host. Respiratory-tract colonization is a key element in the pathogenesis of *M. catarrhalis* infection and remains incompletely understood. Currently available data on age-specific colonization rates indicate that infants are

exposed to *M. catarrhalis* very early in life [4, 5], whereas carriage rates in older children and healthy adults are low [6, 7]. The latter data are difficult to explain for a number of reasons. (1) Because it is an exclusively human pathogen [8], the major source of transmission of *M. catarrhalis* to infants is adults—one would thus expect that early exposure of infants would reflect frequent colonization of their closest contacts; (2) adults demonstrate a robust mucosal IgA response suggestive of frequent or continuous exposure [9]; and (3) the presence of a viral respiratory-tract infection increases the rate of recovery of *M. catarrhalis* from the pharynx [6, 7]. These considerations suggest that colonization might be more frequent than is determined by mucosal surface sampling and that this technique underestimates true carriage rates. We thus postulated the existence of a *M. catarrhalis* reservoir beneath the mucosal surface. This hypothesis was supported by studies demonstrating that the organism can be recovered from homogenized tonsillar core tissue from individuals without acute respiratory-tract infection [10, 11]; that the apical surface of tonsillar epithelia cells expresses carcinoembryonic antigen-related cell adhesion molecules [12], which are targeted by the UspA1

Received 17 January 2007; accepted 3 April 2007; electronically published 30 August 2007.

Potential conflict of interest: none reported.

Financial support: Swiss National Science Foundation (grant 3100A0-102246 to C.A.).

Reprints or correspondence: Dr. Christoph Aebi, Dept. of Pediatrics, University of Bern, Inselspital, CH-3010 Bern, Switzerland (christoph.aebi@insel.ch).

**The Journal of Infectious Diseases** 2007;196:1080–7

© 2007 by the Infectious Diseases Society of America. All rights reserved.

0022-1899/2007/19607-0021\$15.00

DOI: 10.1086/521194

**Table 1. Oligonucleotides used in the study.**

Gene, oligonucleotide	Sequence (5'→ 3')	Use	Reference
<i>uspA1</i>			
uspA1_cT-tgt2F	GTCAAACAGCTGGAGGTATTGC	PCR	[19]
uspA1_cT-tgt2R	GACATGATGCTCACCTGCTCTA	PCR	[19]
uspA1_cT-tgt2M1	(FAM)ATCGCAATTGCAACTTT(TAMRA)	PCR	[19]
<i>16S rRNA</i>			
16S-tgt1F	GGGCGAAAGCCTGATCCA	PCR	Present study
16S-tgt1R	CCATAAGCTTTCTCCCACTT	PCR	Present study
16S-tgt1M2	(FAM)AACCAAAAGGCCTTCTTCA(TAMRA)	PCR	Present study
<i>Mcat</i> -FISH	AGGTCGTATGCGGTATTAGCTTGGGTTTC	FISH	Present study
ns- <i>Mcat</i>	GAAACCCAAGCTAATACCGCATACGACCT	FISH	Present study
EUB338	GCTGCCTCCCGTAGGAGT	FISH	[20]

**NOTE.** F, forward; FAM, 6-carboxyfluorescein; FISH, fluorescent in situ hybridization; PCR, polymerase chain reaction; R, reverse; TAMRA, 6-carboxytetramethylrhodamine.

adhesin [13]; and that *M. catarrhalis* appears to have the potential to invade epithelial cells [14]. In addition, the identification of a subepithelial habitat in lymphoid tissues would provide a rationale for in vitro findings demonstrating that the *M. catarrhalis* IgD-binding protein (MID, also known as hemagglutinin) is capable of inducing polyclonal activation of human B cells [15, 16]. The detection of *M. catarrhalis* in adenoids and tonsils would thus identify an anatomic site where physical interaction between MID and B cells may occur. The aims of the present study were to comprehensively search for the presence of *M. catarrhalis* in tonsillar and adenoidal tissue from individuals undergoing elective surgery and to characterize its tissue distribution.

## MATERIALS AND METHODS

**Tissue collection and preparation.** Tissue samples were obtained from 40 patients undergoing adenoidectomy and/or tonsillectomy performed by one of the authors (M.V.). The study was approved by the ethics committee, and written, informed

consent was obtained from each patient or legal guardian. Indications for surgery included recurrent or chronic otitis media, hearing impairment associated with chronic otitis media with effusion, and obstructive sleep apnea. Immediately after removal, specimens were cut into 4 pieces of equal size, 2 of which were placed in RNAlater (Ambion) and stored at  $-20^{\circ}\text{C}$  until nucleic acid extractions were performed. Samples used for culture and histologic analysis were wrapped in sterile gauze soaked with normal saline and kept on ice. Samples were delivered to the laboratory within 2 h of surgery and processed within 6 h.

**Bacterial culture.** One quarter of each sample was used for selective culture. Specimens were cut into small fragments, resuspended in 1 mL of PBS; plated on Brucella agar (Becton Dickinson) supplemented with 5% sheep blood, amphotericin B, vancomycin, trimethoprim, and acetazolamide [17]; and incubated at  $37^{\circ}\text{C}$  in 5%  $\text{CO}_2$ . *M. catarrhalis* was identified on the basis of gram staining, oxidase testing, cefinase and DNase production, and API NH (bioMérieux).

**Table 2. Detection of *Moraxella catarrhalis* in adenoids and tonsils using different techniques, including culture, *uspA1* real-time DNA polymerase chain reaction (PCR), *16S rRNA* real-time RNA PCR, immunohistochemical analysis (IHC) using monoclonal antibody 17C7, and fluorescent in situ hybridization (FISH).**

Sample type (no.)	Detection method					Any method
	Culture ( <i>n</i> = 52) <sup>a</sup>	DNA PCR ( <i>n</i> = 52) <sup>a</sup>	RNA PCR ( <i>n</i> = 51) <sup>a</sup>	IHC ( <i>n</i> = 49) <sup>a</sup>	FISH ( <i>n</i> = 48) <sup>a</sup>	
Adenoids ( <i>n</i> = 32) <sup>b</sup>	6 (19)	6 (19)	13 (41)	18 (60)	25 (89)	29 (91)
Tonsils ( <i>n</i> = 20) <sup>b</sup>	1 (5)	4 (20)	8 (42)	12 (63)	17 (85)	17 (85)
Any tissue sample ( <i>n</i> = 52) <sup>c</sup>	7 (13)	10 (19)	21 (41)	30 (61)	42 (87)	46 (88)
Patients ( <i>n</i> = 40) <sup>d</sup>	6/40	9/40	19/39	26/38	34/37	37/40

**NOTE.** Data are no. (%) of positive samples, unless otherwise indicated. Because of tissue limitation, assays were not performed on all specimens.

<sup>a</sup> Total no. of tissue specimens examined (adenoids and tonsils).

<sup>b</sup> *P* = .83 (test statistic, 0.002) for comparison of detection rates in adenoids vs. tonsils.

<sup>c</sup> *P* < .001 (test statistic, 42.64) for comparison of methods.

<sup>d</sup> No. positive/no. tested. *P* < .001 (test statistic, 32.32) for comparison of methods.

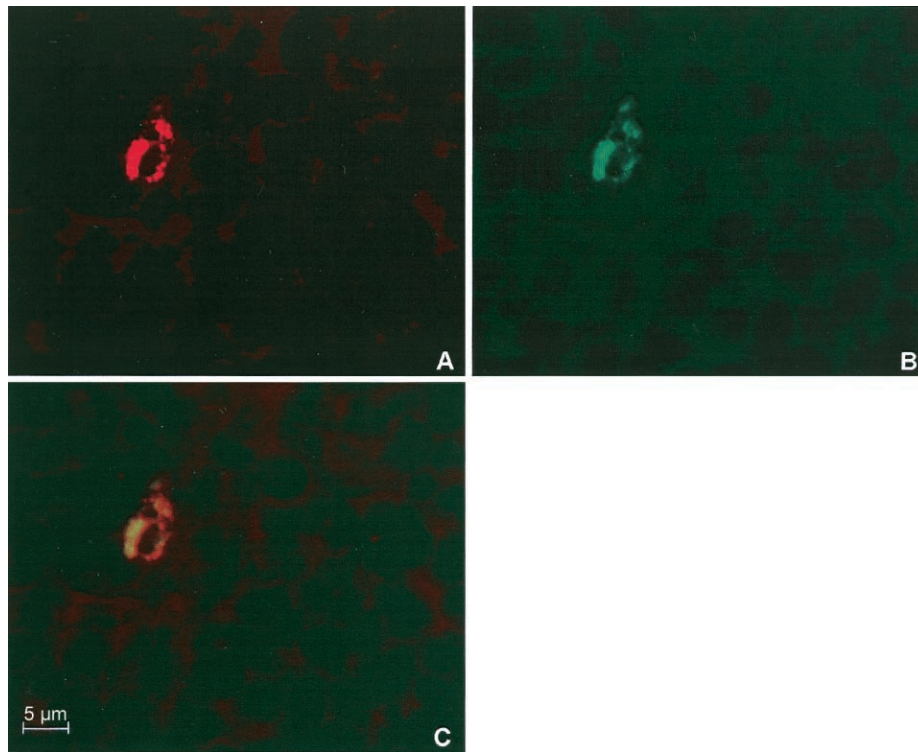


**Figure 1.** Stainings of a cryosection for *Moraxella catarrhalis* by fluorescent in situ hybridization (A) and by immunofluorescence using monoclonal antibody 17C7 (B). The overlay (C) demonstrates colocalization of both signals. Original magnification,  $\times 630$ .

#### **Real-time DNA and RNA polymerase chain reaction (PCR).**

DNA was extracted using the QIAamp DNA Mini Kit (Qiagen). A 25-mg tissue portion was cut into small slices, resuspended in 360  $\mu\text{L}$  of ATL tissue lysis buffer (Qiagen) supplemented with 180  $\mu\text{g}$  of proteinase K (Roche Diagnostics), and incubated at 56°C on a shaking platform until digestion was complete. PCR was designed to target the *uspA1* gene [18, 19]. A 5- $\mu\text{L}$  portion of DNA extract was added to 12.5  $\mu\text{L}$  of 2 $\times$  TaqMan universal PCR master mix (Applied Biosystems), 900 nmol of each primer, and 200 nmol of TaqMan probe (table 1) in a final volume of 25  $\mu\text{L}$ . Thermal cycling conditions were 2 min at 50°C, 10 min at 95°C, and 1 min at 60°C.

For extraction of RNA, specimens were cut into small slices, 800  $\mu\text{L}$  of Trizol Reagent (Life Technologies) was added, and tissue was homogenized using a Teflon pestle tissue homogenizer (Polylabo). Samples were mixed with 200  $\mu\text{L}$  of chloroform, vigorously shaken for 15 s, and centrifuged for 15 min at 13,000 g at 4°C. The supernatant was transferred to 500  $\mu\text{L}$  of lysis buffer, incubated for 5 min at 37°C, and stored at  $-20^\circ\text{C}$  for 1 h. Subsequent extraction was done using the RNeasy Mini kit (Qiagen). RNA was eluted in 50  $\mu\text{L}$  of water and treated with RNase-free DNase I (Invitrogen). Then, 10  $\mu\text{L}$  of extract were subjected to reverse transcription using 0.5  $\mu\text{g}$  of random primers (Catalysis) and SuperScript II (Invitrogen) in accordance with an established protocol [19]. PCR was performed

on ABI Prism 7000 device (Applied Biosystems) using primers and TaqMan probes specific for the 16S *rRNA* gene of *M. catarrhalis* (table 1). Each run included controls for DNA contamination, in that RNA was subjected to the same procedure without the addition of reverse transcriptase. Samples were run in triplicate, and no-template controls were included.

**Immunohistochemical analysis (IHC).** Tissue was embedded in OCT compound (Digitana) and stored at  $-80^\circ\text{C}$ . Six-micron cryosections were prepared (Leica CM1850; Leica Microsystems), placed on microscope slides (SuperFrost Plus; Menzel), and fixed in ice-cold acetone for 20 min. For IHC, *M. catarrhalis* was detected with the *UspA1/2*-specific monoclonal antibody (MAb) 17C7 (1:50) and a goat anti-mouse secondary antibody labeled with Alexa 488 (1:1000; Invitrogen). Epithelial cells were visualized by rabbit anti-human cytokeratin (1:100; Invitrogen) and a Cy3-conjugated goat anti-rabbit antibody (1:1000; Milan Analytica). Actin was labeled with rhodamine phalloidine (8 U/section; Invitrogen). Antibodies against CD1a, CD20, CD14, and CD68 were purchased from Dako (Cytomation). Antibodies were diluted in Tris-buffered saline that contained 0.25% of bovine serum albumin (Sigma-Aldrich). Cryosections were washed in PBS between incubations, placed in a moisture chamber during incubations, counterstained with 4',6'-diamidino-2-phenylindole hydrochloride (DAPI; Sanofi-Aventis), mounted in Mowiol (Calbiochem)

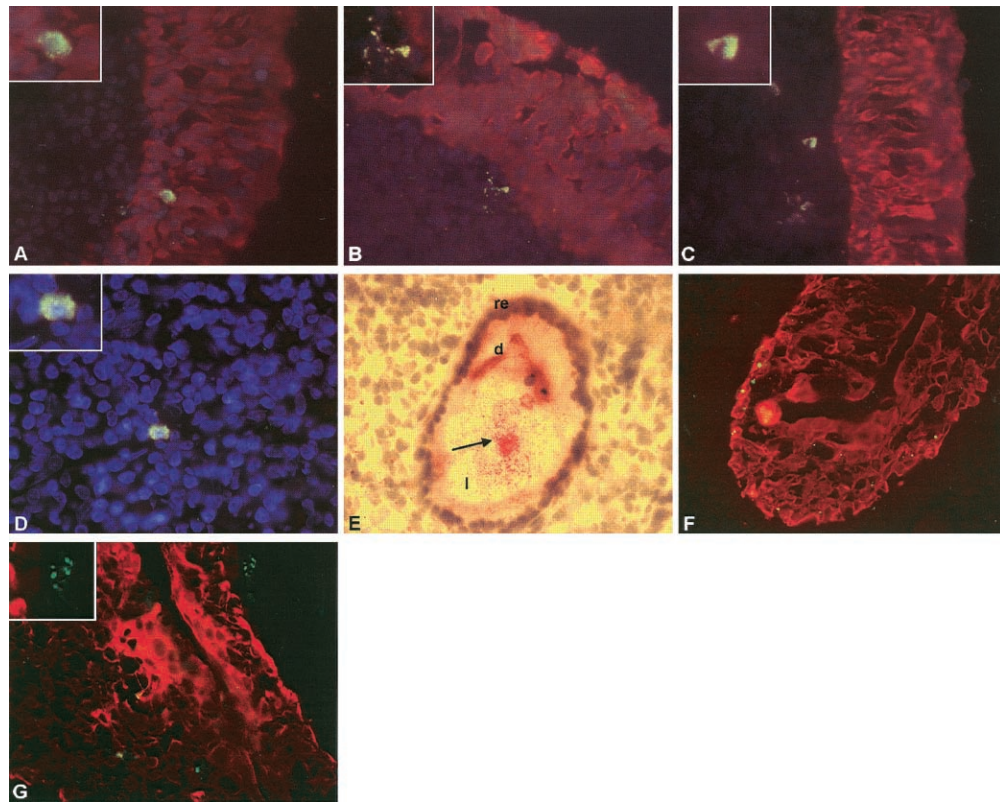


**Figure 2.** Distribution of *Moraxella catarrhalis* in adenoids and tonsils. Infiltration of the surface epithelium (A), subepithelial location of single cells and small conglomerates (B and C), and clusters associated with host cells (C and D) are shown. E, Crypt filled with aggregates of *M. catarrhalis* (arrow; re, reticular epithelium; l, lumen; d, cellular debris). F and G, Bacteria within and beneath the crypt epithelium. Bacteria were visualized by fluorescent in situ hybridization (A–D), immunofluorescence (F and G), or immunoenzymatic staining (E). Red, epithelium labeled with anti-human cytokeratin; blue, 4',6'-diamidino-2-phenylindole hydrochloride-stained nuclei. Original magnifications,  $\times 630$ , except in panel E ( $\times 400$ ). Insets are enlargements of the region of interest.

supplemented with 2.5% DABCO (Fluka), and viewed using a fluorescence microscope (Axiophot Zeiss). Immunoenzymatic stainings were done using the Dako double-stain EnVision system. Sections were counterstained with Mayer's hematoxylin (Sigma-Aldrich) and embedded in Faramount Aqueous Mounting Medium (Dako).

**Fluorescent in situ hybridization (FISH).** Six-micron tissue cryosections placed on SuperFrost Plus microscope slides were fixed with fresh 4% paraformaldehyde in PBS at room temperature for 20 min. Slides were subsequently rinsed in PBS. Sections were hybridized with 0.3 nmol/ $\mu$ L each of *M. catarrhalis*-FISH, a 5' fluorescein isothiocyanate-labeled 16S rRNA probe (bp 118–147) specific for *M. catarrhalis*, and the 5' Cy3-labeled control probe EUB338 (MWG Biotech). EUB338 targets a conserved domain of bacterial 16S rRNA [20]. Probes were diluted in 150  $\mu$ L of hybridization buffer (0.02 mol/L Tris-HCl [pH 8.0], 0.9 mol/L NaCl, 0.01% SDS, and 30% formamide), and hybridization was performed overnight at room temperature in a humid chamber in the dark. To remove excess probe, sections were washed in washing solution for 20 min at 48°C,

rinsed in water, counterstained with DAPI, washed in PBS, mounted in Mowiol-DABCO 2.5%, and examined using a fluorescence microscope.

**Confocal laser scanning microscopy (CLSM).** Sections were subjected to FISH as described above. Actin was visualized by rhodamine phalloidine (Invitrogen). Sections were scanned under a 63 $\times$  oil-immersion objective using a Zeiss LSM 510 Meta confocal microscope with an inverted Zeiss microscope (Axiovert 200M). The z-stacks were reconstructed into z-projections using LSM software (version 3.2; Zeiss).

**Statistical analysis.** Homogeneity of Poisson rates (exact test) was used for comparing the methods of detection of *M. catarrhalis* in tissue sections (StatXact version 6.2; Cytel).

## RESULTS

**Comparison of culture, DNA PCR, RNA PCR, IHC, and FISH for detection of *M. catarrhalis* in adenoids and tonsils.** Thirty-two adenoids and 20 tonsils from 40 patients (median age, 7.1 years; range, 2.1–29.0 years) were studied (table



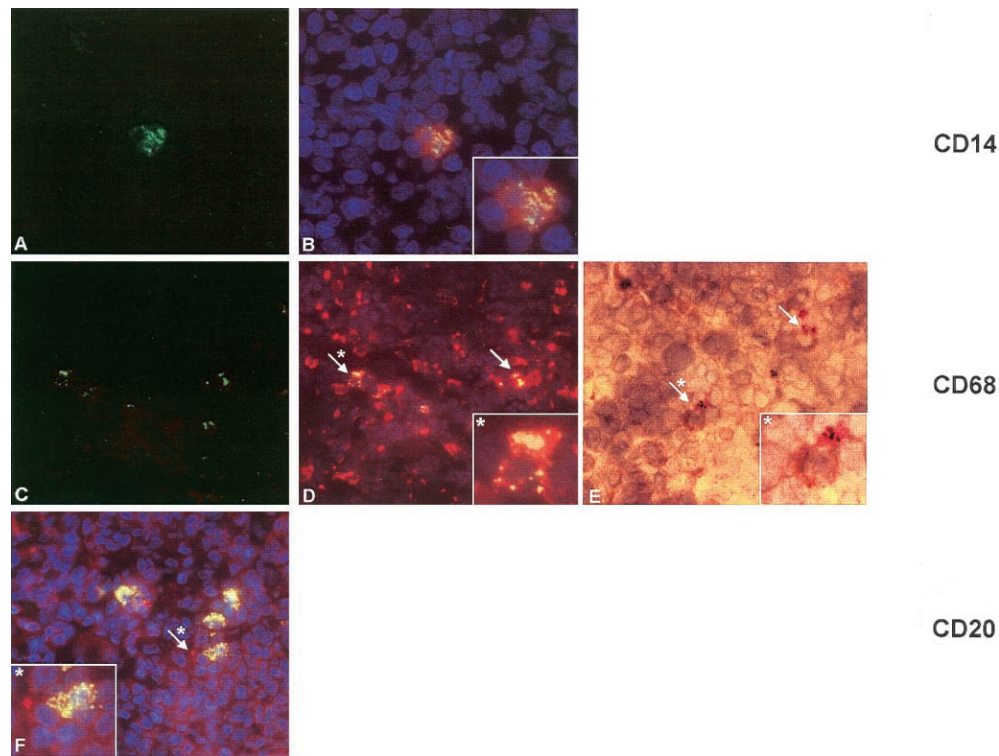


**Figure 3.** Double-stained sections showing *Moraxella catarrhalis* associated with macrophages and B cells. *A* and *B*, Bacteria stained using fluorescent in situ hybridization (FISH) (*A*) and colocalization with CD14<sup>+</sup> cells (*B*, yellow overlay signal). *C* and *D*, Colocalization of *M. catarrhalis* (*C*) and CD68<sup>+</sup> cells (*D*, yellow overlay signal). *E*, Association of bacteria (red) with CD68<sup>+</sup> cells (brown), determined using immunoenzymatic staining. *F*, *M. catarrhalis* interacting with B cells (overlay signal generated by *M. catarrhalis*–FISH probe and CD20 reactivity). Sections were double stained for *M. catarrhalis* (green) and CD14, CD68, or CD20 using monoclonal antibodies and Cy3-conjugated secondary antibodies (red), resulting in a yellow overlay signal. Original magnification,  $\times 630$ .

2). Overall, *M. catarrhalis* was detected in 37 patients (93%). Culture was positive in 7 specimens (13%). Colony-forming units recovered varied between  $3 \times 10^1$  and  $2 \times 10^3$  cfu/300 mg of tissue. All culture-positive specimens and 3 culture-negative samples were positive in DNA PCR (19%). Because of tissue limitation, RNA extractions and histologic analysis could not be performed on all specimens. RNA PCR was positive in 21 (41%) of 51 samples. IHC and FISH detected *M. catarrhalis* in 30 (61%) of 49 and 42 (88%) of 48 specimens, respectively. All samples but one that tested positive in RNA PCR or IHC were positive when tested by FISH. FISH was the most sensitive technique ( $P < .001$ ).

**Specificity of FISH.** The specificity of the FISH probe was evaluated as follows. (1) It was designed to be complementary to a specific and conserved region of the 16S *rRNA* gene, and a National Center for Biotechnology Information gene bank BLAST search failed to identify homologous sequences. (2) *M. catarrhalis* whole cells of all three 16S *rRNA* types were detected with equal signal intensity. No cross-hybridization to any of the following species was observed: *M. phenylpyruvica*, *M. osloensis*, *M. nonliquefaciens*, *Pseudomonas aeruginosa*, *Bordetella pertussis*, *Haemophilus influenzae*, *Streptococcus pneumoniae*, *S.*

*pyogenes*, *Staphylococcus aureus*, *Neisseria lactamica*, *N. meningitidis* serogroups B and C, *N. gonorrhoeae*, *Acinetobacter calcoaceticus*, *A. baumannii*, and *A. lwoffii* (data not shown). (3) The unlabeled probe ns-*Mcat* (table 1), which is complementary to the *M. catarrhalis* 16S *rRNA* gene target sequence but lacks a fluorescent tag, was added to sections before FISH. The absence of a fluorescent signal excluded the possibility of non-specific binding of the fluorescent dye. (4) Figure 1 shows a section that was double stained by FISH (figure 1A) and MAb 17C7 (figure 1B). The yellow color in the overlay (figure 1C) indicates that both signals colocalized.

**Histologic location of *M. catarrhalis*.** Sections showed a characteristic tissue distribution of *M. catarrhalis* (figure 2). Both types of epithelia, the respiratory epithelium lining the adenoids and the stratified squamous epithelium of the tonsils, were invaded by *M. catarrhalis* diffusely, in linear, transepithelial tracts (not shown) or in clusters associated with host cells (figure 2A). Double staining for *M. catarrhalis* and keratin for visualization of the epithelial layer demonstrated fluorescent bacteria located beneath the epithelium within the lamina propria (figure 2B and 2C). *M. catarrhalis* was consistently found in the subepithelial region of all positive tissues and typically

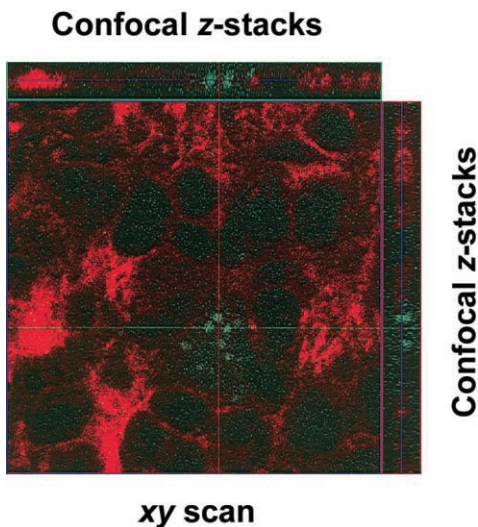


**Figure 4.** Demonstration of intracellular *Moraxella catarrhalis* by confocal laser scanning microscopy. The image is a projection of 3- $\mu\text{m}$  z-stacks collected through the 630 $\times$  objective on a confocal microscope. A cluster of *M. catarrhalis* (green) is shown, and actin was visualized by rhodamine phalloidine (red).

formed conglomerates associated with host cells and sparing their nuclei (figure 2C and 2D). In heavily infiltrated areas, up to 15 visual fields with fluorescent bacteria were counted, when sections were screened at  $\times 400$ . Areas with high densities of *M. catarrhalis* were observed in corresponding regions of consecutive serial sections, which ruled out contamination during the cutting procedure. In some sections, crypts were filled with large numbers of bacteria (figure 2E). In these locations, single bacteria and small clusters were also seen within and beneath the reticular crypt epithelium, respectively (figure 2F and 2G). These findings provide evidence that *M. catarrhalis* penetrates both the surface and crypt epithelia.

**Association of *M. catarrhalis* with immune cells.** Five heavily colonized tissue specimens were stained for immunophenotypic markers. We used monoclonal antibodies specific for CD14 and CD68 to stain cells of the monocyte/macrophage lineage, CD20 to visualize B cells, and CD1a to label dendritic cells. In all samples examined, subepithelial clusters of *M. catarrhalis* were mainly associated with CD14<sup>+</sup> and CD68<sup>+</sup> cells. Colocalizations with macrophages are shown in figure 3, both by FISH combined with immunofluorescent staining (figure 3A–3D) and by immunoenzymatic staining (figure 3E). Labeling of B cells demonstrated that clusters of *M. catarrhalis* were located in the extrafollicular region and, occasionally, in the outer mantle zone of lymphoid follicles, where they were seen adjacent to CD20<sup>+</sup> cells (figure 3F). No bacteria were detected in the germinal center, and no association was found with CD1a<sup>+</sup> cells.

**Intracellular location of *M. catarrhalis*.** The findings pre-

sented above suggested that *M. catarrhalis* is able to reside intracellularly. We used CLSM to demonstrate that bacteria seen in the intra- and subepithelial region were indeed located within eukaryotic cells. In figure 4, *M. catarrhalis* was immunostained (green), and actin was labeled by rhodamine phalloidine to visualize cytoplasmic structure (red). Confocal *xy* scans (0.3  $\mu\text{m}$ ) were taken along the *z*-axis. To illustrate that bacteria resided within host cell, projections shown in the top and right image were constructed from confocal *z*-stacks.

## DISCUSSION

Adenoids and tonsils play a key role in antigen sampling and immune response induction directed against respiratory pathogens. Some organisms, however (e.g., *H. influenzae* [21, 22] *S. pyogenes* [23], and *S. aureus* [24]), deploy mechanisms to use pharyngeal lymphoid tissues as a niche to persist in the host.

Here we have demonstrated that adenoids and tonsils from patients without acute respiratory-tract disease harbor a subepithelial and intracellular reservoir of *M. catarrhalis*. Identification and histologic localization of bacteria depended largely on IHC and FISH analysis, the latter of which was positive in 89% and 85% of adenoids and tonsils, respectively. These figures are greater than what would be expected from pharyngeal surface sampling in asymptomatic individuals >2 years old [6, 7] and emphasize that colonization with *M. catarrhalis* may be much more prevalent than has been previously appreciated. We concede that the proportion of patients carrying viable bacteria may be lower and that those who undergo surgery may not be fully representative of a healthy population. In any event, however, our findings demonstrate that the mucosal surface is not the only habitat of *M. catarrhalis* and that carriage is underestimated by surface culture. Thus, growth from a standard pharyngeal surface culture may reflect a certain minimal density of the organism at the time of sampling rather than the presence or absence of carriage per se. The implications of this concept are manifold. First, if the majority of individuals are continuously colonized, both long-term maintenance of immunity [9] and early exposure of infants [4] are plausible. Second, the increase in recovery of *M. catarrhalis* during episodes of the common cold [25] may not necessarily reflect de novo acquisition but may be explained by the expansion of a resident pool of bacteria [26, 27]. The observation that consecutive episodes of colonization often are caused by different strains [28, 29] does not rule out such a scenario, because the tissue reservoir might be multiclonal. On the basis of these considerations, one may ask why some hosts allow expansion to high densities with, consequently, an increased risk of symptomatic infection such as acute otitis media [1], whereas others do not. This would be another approach for studying the enigma of “otitis-prone” children. Alternatively, one might postulate that chronic car-

riage of *M. catarrhalis* identifies chronically symptomatic individuals and explains the occurrence of entities such as recurrent otitis media and adenotonsillar hypertrophy.

We used an exhaustive array of detection techniques for tracking a single pathogen in a mucosa-associated organ, an approach that, to our knowledge, has not been previously reported. The low recovery rate by culture (13%) might reflect low bacterial density, impaired growth capacity of intratonsillar bacteria (e.g., auxotrophic intracellular persisters), or our use of a selective medium. It appears likely that culture substantially underestimated the presence of viable bacteria, because 41% of samples were RNA PCR positive. The discrepancy between DNA PCR (19%) and FISH (87%) results is more difficult to explain, but it should be noted that the former was not optimized to reduce the potential effect of tissue polymerase inhibitors. On the basis of previous experience with large collections of clinical isolates of *M. catarrhalis* [30], it is highly unlikely that the PCR primers targeted insufficiently conserved DNA sequences.

Our findings present the first in vivo evidence that *M. catarrhalis* has the potential to penetrate the epithelial barrier and reside intracellularly. Previously considered an extracellular pathogen, it has now been shown to invade respiratory epithelial cells in vitro and appears to actively induce this process [14]. Invasion is a strategy employed by several species—including *H. influenzae* [31], *S. pneumoniae* [32], *Mycobacterium tuberculosis* [33], *Listeria monocytogenes* [34], and *S. aureus* [35]—to evade contact with antimicrobial peptides, pattern-recognition receptors, antibodies, and other effectors of the host defense. Subepithelial and intracellular location may thus explain the survival of *M. catarrhalis* in the presence of mucosal IgA [9], bactericidal serum IgG [36], and defensins [37].

We found large conglomerates of *M. catarrhalis* in the lumen of crypts (figure 2E), an observation previously described for other species [22, 38]. There is evidence to suggest that intracryptal bacterial conglomerates produce biofilms [39], which provide protection against the host defense and antimicrobial agents. However, available evidence suggests that biofilm formation by *M. catarrhalis* in vitro is variable and strain dependent [40], and its importance in vivo is unclear. Differential expression of cytokeratins and glycoconjugates in reticular crypt epithelium and the surface epithelium [41] explains why some bacteria exhibit preferential binding to these respective regions. Our stainings visualized that *M. catarrhalis* crosses crypt epithelia (figure 2F and 2G), which are enriched for M cells [42]. This finding suggests that M cells may be engaged in the trans-epithelial transport of this organism.

Confocal microscopy established that some *M. catarrhalis* cells reside intracellularly (figure 4) and that clusters of bacteria colocalize with macrophages in the lamina propria (figure 3A–3D). Nontypeable *H. influenzae* is similarly distributed in ad-

enoids [21, 22] and was previously shown to be able to persist in macrophages [21, 22]. The intracellular fate of *M. catarrhalis* is unknown at present. The fact that invasion, survival, and persistence in macrophages is a strategy used by a number of other respiratory pathogens (e.g., *B. pertussis* [43], *P. aeruginosa* [44], and *Burkholderia cepacia* [45]), that intracellular *M. catarrhalis* survives for at least 6 h in vitro, and that it is located in a protected area within macropinosomes [14] allow the assumption that it might behave similarly.

Finally, we provide evidence that *M. catarrhalis* physically interacts with B cells in the outer mantle zone of lymphoid follicles, where mainly naive B cells reside (figure 3). In vitro studies have demonstrated that *M. catarrhalis* has the unique characteristic to stimulate human B cells through the high affinity of the MID/hemagglutinin outer-membrane protein with surface-bound IgD. This interaction leads to clonal expansion of B cells in vitro and induces antibody production [16, 46]. It is thus conceivable that the interaction between *M. catarrhalis* and B cells in vivo contributes to the maintenance of long-term humoral immunity and might promote adenotonsillar hyperplasia in children.

In summary, we have demonstrated that *M. catarrhalis* could be detected in tissue from >90% of individuals who underwent elective tonsillectomy and/or adenoidectomy and that these lymphoid tissues provide a subepithelial and intracellular niche, which is not accessible to pharyngeal surface sampling and which might be a source of endogenous reinfection.

## Acknowledgments

We thank Dr. Eric Hansen, Department of Microbiology, University of Texas Southwestern Medical Center, Dallas, for providing the monoclonal antibody 17C7, and Dr. Roland A. Ammann, Department of Pediatrics, University of Bern, Switzerland, for statistical support.

## References

1. Revai K, McCormick DP, Patel J, Grady JJ, Saeed K, Chonmaitree T. Effect of pneumococcal conjugate vaccine on nasopharyngeal bacterial colonization during acute otitis media. *Pediatrics* **2006**; 117:1823–9.
2. Block SL, Hedrick J, Harrison CJ, et al. Community-wide vaccination with the heptavalent pneumococcal conjugate significantly alters the microbiology of acute otitis media. *Pediatr Infect Dis J* **2004**; 23:829–33.
3. Hays JP, van der Schee C, Loogman A, et al. Total genome polymorphism and low frequency of intra-genomic variation in the *uspA1* and *uspA2* genes of *Moraxella catarrhalis* in otitis prone and non-prone children up to 2 years of age: consequences for vaccine design? *Vaccine* **2003**; 21: 1118–24.
4. Meier PS, Freiburghaus S, Martin A, Heiniger N, Troller R, Aebi C. Mucosal immune response to specific outer membrane proteins of *Moraxella catarrhalis* in young children. *Pediatr Infect Dis J* **2003**; 22:256–62.
5. Leach AJ, Boswell JB, Asche V, Nienhuys TG, Mathews JD. Bacterial colonization of the nasopharynx predicts very early onset and persistence of otitis media in Australian aboriginal infants. *Pediatr Infect Dis J* **1994**; 13:983–9.
6. Ejertsen T, Thisted E, Ebbesen F, Olesen B, Renneberg J. A study of

- prevalence, time of colonisation, and association with upper and lower respiratory tract infections. *J Infect* **1994**; 29:23–31.
7. Lieberman D, Shleyfer E, Castel H, et al. Nasopharyngeal versus oropharyngeal sampling for isolation of potential respiratory pathogens in adults. *J Clin Microbiol* **2006**; 44:525–8.
  8. Bowers LC, Purcell JE, Plauche GB, Denoel PA, Lobet Y, Philipp MT. Assessment of the nasopharyngeal bacterial flora of rhesus macaques: *Moraxella*, *Neisseria*, *Haemophilus*, and other genera. *J Clin Microbiol* **2002**; 40:4340–2.
  9. Stutzmann Meier P, Heiniger N, Troller R, Aebi C. Salivary antibodies directed against outer membrane proteins of *Moraxella catarrhalis* in healthy adults. *Infect Immun* **2003**; 71:6793–8.
  10. Brook I, Shah K, Jackson W. Microbiology of healthy and diseased adenoids. *Laryngoscope* **2000**; 110:994–9.
  11. Eliasson I, Kamme C, Prellner K. Beta-lactamase production in the upper respiratory tract flora. *Eur J Clin Microbiol* **1986**; 5:507–12.
  12. Virji M. CEA and innate immunity. *Trends Microbiol* **2001**; 9:258–9.
  13. Hill DJ, Virji M. A novel cell-binding mechanism of *Moraxella catarrhalis* ubiquitous surface protein UspA: specific targeting of the N-domain of carcinoembryonic antigen-related cell adhesion molecules by UspA1. *Mol Microbiol* **2003**; 48:117–29.
  14. Slevogt H, Seybold J, Tiwari KN, et al. *Moraxella catarrhalis* is internalized in respiratory epithelial cells by a trigger-like mechanism and initiates a TLR2- and partly NOD1-dependent inflammatory immune response. *Cell Microbiol* **2007**; 9:694–707.
  15. Gyorloff WA, Hadzic R, Forsgren A, Riesbeck K. The novel IgD binding protein from *Moraxella catarrhalis* induces human B lymphocyte activation and Ig secretion in the presence of Th2 cytokines. *J Immunol* **2002**; 168:5582–8.
  16. Nordstrom T, Jendholm J, Samuelsson M, Forsgren A, Riesbeck K. The IgD-binding domain of the *Moraxella* IgD-binding protein MID (MID962-1200) activates human B cells in the presence of T cell cytokines. *J Leukoc Biol* **2006**; 79:319–29.
  17. Vanechoutte M, Verschraegen G, Claeys G, Van den Abeele AM. Selective medium for *Branhamella catarrhalis* with acetazolamide as a specific inhibitor of *Neisseria* spp. *J Clin Microbiol* **1988**; 26:2544–8.
  18. Meier PS, Troller R, Heiniger N, Grivea IN, Syrogiannopoulos GA, Aebi C. *Moraxella catarrhalis* strains with reduced expression of the UspA outer membrane proteins belong to a distinct subpopulation. *Vaccine* **2005**; 23:2000–8.
  19. Heiniger N, Troller R, Meier PS, Aebi C. Cold shock response of the UspA1 outer membrane adhesin of *Moraxella catarrhalis*. *Infect Immun* **2005**; 73:8247–55.
  20. Amann RI, Binder BJ, Olson RJ, Chisholm SW, Devereux R, Stahl DA. Combination of 16S rRNA-targeted oligonucleotide probes with flow cytometry for analyzing mixed microbial populations. *Appl Environ Microbiol* **1990**; 56:1919–25.
  21. Forsgren J, Samuelson A, Ahlin A, Jonasson J, Rynnel-Dagoo B, Lindberg A. *Haemophilus influenzae* resides and multiplies intracellularly in human adenoid tissue as demonstrated by in situ hybridization and bacterial viability assay. *Infect Immun* **1994**; 62:673–9.
  22. Forsgren J, Samuelson A, Borrelli S, Christensson B, Jonasson J, Lindberg AA. Persistence of nontypeable *Haemophilus influenzae* in adenoid macrophages: a putative colonization mechanism. *Acta Otolaryngol* **1996**; 116:766–73.
  23. Podbielski A, Beckert S, Schattke R, et al. Epidemiology and virulence gene expression of intracellular group A streptococci in tonsils of recurrently infected adults. *Int J Med Microbiol* **2003**; 293:179–90.
  24. Clement S, Vaudaux P, Francois P, et al. Evidence of an intracellular reservoir in the nasal mucosa of patients with recurrent *Staphylococcus aureus* rhinosinusitis. *J Infect Dis* **2005**; 192:1023–8.
  25. Korppi M, Katila ML, Jaaskelainen J, Leinonen M. Role of *Moraxella (Branhamella) catarrhalis* as a respiratory pathogen in children. *Acta Paediatr* **1992**; 81:993–6.
  26. Groeneveld K, van Alphen L, Eijk PP, Visschers G, Jansen HM, Zanen HC. Endogenous and exogenous reinfections by *Haemophilus influenzae* in patients with chronic obstructive pulmonary disease: the effect of antibiotic treatment on persistence. *J Infect Dis* **1990**; 161:512–7.
  27. Samuelson A, Freijd A, Jonasson J, Lindberg AA. Turnover of nonencapsulated *Haemophilus influenzae* in the nasopharynx of otitis-prone children. *J Clin Microbiol* **1995**; 33:2027–31.
  28. Faden H, Harabuchi Y, Hong JJ. Epidemiology of *Moraxella catarrhalis* in children during the first 2 years of life: relationship to otitis media. *J Infect Dis* **1994**; 169:1312–7.
  29. Klingman KL, Pye A, Murphy TF, Hill SL. Dynamics of respiratory tract colonization by *Branhamella catarrhalis* in bronchiectasis. *Am J Respir Crit Care Med* **1995**; 152:1072–8.
  30. Meier PS, Troller R, Grivea IN, Syrogiannopoulos GA, Aebi C. The outer membrane proteins UspA1 and UspA2 of *Moraxella catarrhalis* are highly conserved in nasopharyngeal isolates from young children. *Vaccine* **2002**; 20:1754–60.
  31. Ahren IL, Williams DL, Rice PJ, Forsgren A, Riesbeck K. The importance of a  $\beta$ -glucan receptor in the nonopsonic entry of nontypeable *Haemophilus influenzae* into human monocytic and epithelial cells. *J Infect Dis* **2001**; 184:150–8.
  32. Talbot UM, Paton AW, Paton JC. Uptake of *Streptococcus pneumoniae* by respiratory epithelial cells. *Infect Immun* **1996**; 64:3772–7.
  33. Mehta PK, King CH, White EH, Murtagh JJ Jr, Quinn FD. Comparison of in vitro models for the study of *Mycobacterium tuberculosis* invasion and intracellular replication. *Infect Immun* **1996**; 64:2673–9.
  34. Drevets DA, Sawyer RT, Potter TA, Campbell PA. *Listeria monocytogenes* infects human endothelial cells by two distinct mechanisms. *Infect Immun* **1995**; 63:4268–76.
  35. Jett BD, Gilmore MS. Internalization of *Staphylococcus aureus* by human corneal epithelial cells: role of bacterial fibronectin-binding protein and host cell factors. *Infect Immun* **2002**; 70:4697–700.
  36. Chen D, Barniak V, Vandermeid KR, McMichael JC. The levels and bactericidal capacity of antibodies directed against the UspA1 and UspA2 outer membrane proteins of *Moraxella (Branhamella) catarrhalis* in adults and children. *Infect Immun* **1999**; 67:1310–6.
  37. Lee HY, Andalibi A, Webster P, et al. Antimicrobial activity of innate immune molecules against *Streptococcus pneumoniae*, *Moraxella catarrhalis* and nontypeable *Haemophilus influenzae*. *BMC Infect Dis* **2004**; 4: 12.
  38. Ebenfelt A, Ericson LE, Lundberg C. Acute pharyngotonsillitis is an infection restricted to the crypt and surface secretion. *Acta Otolaryngol* **1998**; 118:264–71.
  39. Chole RA, Faddis BT. Anatomical evidence of microbial biofilms in tonsillar tissues: a possible mechanism to explain chronicity. *Arch Otolaryngol Head Neck Surg* **2003**; 129:634–6.
  40. Pearson MM, Laurence CA, Guinn SE, Hansen EJ. Biofilm formation by *Moraxella catarrhalis* in vitro: roles of the UspA1 adhesin and the Hag hemagglutinin. *Infect Immun* **2006**; 74:1588–96.
  41. Clark MA, Wilson C, Sama A, Wilson JA, Hirst BH. Differential cytokeratin and glycoconjugate expression by the surface and crypt epithelia of human palatine tonsils. *Histochem Cell Biol* **2000**; 114:311–21.
  42. Howie AJ. Scanning and transmission electron microscopy on the epithelium of human palatine tonsils. *J Pathol* **1980**; 130:91–8.
  43. Friedman RL, Nordensson K, Wilson L, Akporiaye ET, Yocum DE. Uptake and intracellular survival of *Bordetella pertussis* in human macrophages. *Infect Immun* **1992**; 60:4578–85.
  44. Mahenthiralingam E, Campbell ME, Speert DP. Nonmotility and phagocytic resistance of *Pseudomonas aeruginosa* isolates from chronically colonized patients with cystic fibrosis. *Infect Immun* **1994**; 62:596–605.
  45. Martin DW, Mohr CD. Invasion and intracellular survival of *Burkholderia cepacia*. *Infect Immun* **2000**; 68:24–9.
  46. Hadzic R, Forsgren A, Cardell LO, Riesbeck K, Wingren AG. The CD19 molecule is crucial for MID-dependent activation of tonsillar B cells from children. *Scand J Immunol* **2005**; 61:165–72.